ORIGINAL RESEARCH

Physiological Assessment of Ventricular Myocardial Voltage Using Omnipolar Electrograms

Karl Magtibay, MASc; Stéphane Massé, MASc; John Asta; Marjan Kusha, MEng; Patrick F. H. Lai, MSc; Mohammed Ali Azam, MBBS, PhD; Andreu Porta-Sanchez, MD; Shouvik Haldar, MD (Res), MRCP; Daniel Malebranche, MD; Christopher Labos, MD; D. Curtis Deno, MD, PhD; Kumaraswamy Nanthakumar, MD, FRCPC

***Background*—**Characterization of myocardial health by bipolar electrograms are critical for ventricular tachycardia therapy. Dependence of bipolar electrograms on electrode orientation may reduce reliability of voltage assessment along the plane of arrhythmic myocardial substrate. Hence, we sought to evaluate voltage assessment from orientation-independent omnipolar electrograms.

***Methods and Results*—**We mapped the ventricular epicardium of 5 isolated hearts from each species—healthy rabbits, healthy pigs, and diseased humans—under paced conditions. We derived bipolar electrograms and voltage peak-to-peak (Vpps) along 2 bipolar electrode orientations (horizontal and vertical). We derived omnipolar electrograms and Vpps using omnipolar electrogram methodology. Voltage maps were created for both bipoles and omnipole. Electrode orientation affects the bipolar voltage map with an average absolute difference between horizontal and vertical of 0.25±0.18 mV in humans. Vpps provide larger absolute values than horizontal and vertical bipolar Vpps by 1.6 and 1.4 mV, respectively, in humans. Bipolar electrograms with the largest Vpps from either along horizontal or vertical orientation are highly correlated with omnipolar electrograms and with Vpps values (0.97±0.08 and 0.94±0.08, respectively). Vpps values are more consistent than bipoles, in both beat-by-beat (CoV, 0.28±0.19 versus 0.08±0.13 in human hearts) and rhythm changes (0.55±0.21 versus 0.40±0.20 in porcine hearts).

***Conclusions*—**Omnipoles provide physiologically relevant and consistent voltages that are along the maximal bipolar direction on the plane of the myocardium. **(*J Am Heart Assoc*. 2017;6:e006447. DOI: 10.1161/JAHA.117.006447.)**

Key Words: electrophysiology mapping • omnipole • physiology • ventricular myocardium • ventricular tachycardia • voltage mapping

During ventricular tachycardia ablation, bipolar electrogram voltage amplitude is widely used for myocardial substrate characterization and for determining relevant therapeutic strategies.[1–5] Josephson and Anter recently highlighted the pitfalls of interpreting bipolar electrogram voltages as a medium for substrate mapping by identifying myriad factors that significantly affect its measurement.[6,7] These factors can be classified into those that can and cannot be standardized. Interelectrode distance and electrode size,[8,9] signal filter settings,[10] and contact force[11] can be standardized by using established mapping tools and recording system settings. Bipolar measurements could yield numerous variations of electrogram morphology and amplitude because of its dependence on electrode orientation with respect to activation direction, which may lead to physiologically ambiguous characterization of the myocardium.[6] Consequently, bipolar voltage maps may not only display significant heterogeneity but are also not reproducible. Therefore, electrograms along the maximal bipole direction that are electrode orientation–independent may yield more physiologically representative parameters of the myocardium compared with traditional bipolar electrograms.

Ideally, to survey a myocardial area for the largest bipolar Vpp, one would have to align a sensing catheter along the estimated activation direction following the creation of local activation time maps or rotate a mapping catheter 360

From the Hull Family Cardiac Fibrillation Management Laboratory, Toronto General Hospital, University Health Network, Toronto, Ontario, Canada (K.M., S.M., J.A., M.K., P.F.H.L., M.A.A., A.P.-S., S.H., D.M., K.N.); McGill University Health Centre, Montreal, Quebec, Canada (C.L.); Abbott, St. Paul, MN (D.C.D.).

A previous abstract of this work was presented at the American Heart Association's Scientific Sessions, November 12–16, 2016, in New Orleans, LA.

Correspondence to: Kumaraswamy Nanthakumar, MD, FRCPC, The Hull Family Cardiac Fibrillation Management Laboratory, Toronto General Hospital, University Health Network, 200 Elizabeth St, GW3-526, Toronto, Ontario, Canada M5G 2C4. E-mail: kumar.nanthakumar@uhn.ca

Received April 21, 2017; accepted June 21, 2017.

© 2017 The Authors. Published on behalf of the American Heart Association, Inc., by Wiley. This is an open access article under the terms of the Creative Commons Attribution-NonCommercial License, which permits use, distribution and reproduction in any medium, provided the original work is properly cited and is not used for commercial purposes.

Clinical Perspective

What Is New?

- Omnipolar mapping technology (OT) utilizes electrogram signals from a regularly spaced array of electrodes and multiple directions to assess the myocardium independent of catheter orientation.
- Working with rabbit, porcine, and human ventricles, omnipolar-derived measurements of peak-to-peak voltage, OT_{Vmax}, were compared with traditional bipolar voltages.
- Compared with local bipoles, local OT_{Vmax} was more reliable and reproducible. In addition, OT_{Vmax} provided greater peak-to-peak voltages than bipoles.
- Using a scar threshold of 1.5 mV, OT_{Vmax}-defined scar area corresponded better to electrophysiologist-determined scar than area determined from bipolar signals.
- Using a lesion gap example, OT_{Vmax} better delineated the gap than maps that relied on catheter bipoles.

What Are the Clinical Implications?

- Obtained with fixed-spacing grid array catheters, omnipolar voltages may rapidly provide reproducible, catheter orientation independent, and reliable substrate characterization.
- Omnipolar voltages may better delineate areas with preserved voltage and conduction by avoiding the tendency of unaligned bipoles to underreport voltage.
- If implemented in 3-dimensional electroanatomical mapping systems, omnipolar voltages may provide more physiologically relevant substrate characterization and thus better direct catheter ablation of ventricular tachycardia.

degrees within that area until the bipolar electrogram with the largest Vpp is obtained. The former would require a priori knowledge of the wavefront's direction, and catheter orientation, while feasible, is time consuming and the latter requires pivoting a catheter at the same time as maintaining electrode contact on the myocardium, and recording innumerable bipoles would be a challenging feat. These methods are impractical to perform in a clinical setting.

Omnipolar electrogram methodology (OT), which was recently introduced by Deno et al[12] and validated by Massé et al,[13] is a potential practical solution to this problem. OT employs multiple electrodes and mathematical models of wave propagation to determine the direction of a traveling wave (TW) along the myocardial plane by interrogating its electric field (E-field). More importantly, OT can survey all possible bipolar electrode orientations without the need for catheter rotation or prior local activation time maps. Therefore, we can use OT to obtain electrode orientation–independent electrogram (OT_{egm}) that is along the maximal bipolar direction. We postulate that such a bipolar electrogram will also have the largest voltage (OT_{Vmax}) compared with any bipole measured along any orientation. In this article, we evaluate the potential use of OT to provide nonambiguous, reproducible, physiologically based assessment of the myocardium.

Specifically, we compared voltage maps created from traditional bipolar electrograms, from predefined orthogonal bipolar electrode orientations, against voltage maps created from omnipoles, OT_{egm} and OT_{Vmax}. We hypothesized that voltage maps created using OT_{Vmax} values have larger amplitude values and have more consistent voltage values, compared with traditional bipolar electrogram Vpps because of its electrode orientation independence. We explored the potential clinical use of OT_{Vmax} in assessing for local physiology of the ventricular myocardium in the presence of radiofrequency lesions.

Methods

We mapped the epicardium of the ventricles of 5 isolated healthy rabbit and porcine hearts in a Langendorff setup to optimize our electrical mapping protocol. We also mapped the epicardium of the ventricles of 5 isolated, ablated porcine hearts and isolated human hearts to test our hypothesis on radiofrequency-ablated and naturally diseased tissues, respectively. All hearts were mapped under a paced condition. Rabbit and porcine heart studies were approved by the Animal Care Committee at Toronto General Hospital (Toronto, ON, Canada). Human heart experiments were separately approved by University Health Network research ethics board (Toronto, ON, Canada) with informed consent obtained from each patient.

Two-Dimensional Electrode Arrays—High-Density Grids and High-Density Plaque

We obtained unipolar electrograms using 3 high-density (HD) 2-dimensional (2D) electrode arrays: HD grids, 16 and 56, and HD plaque. The HD 16 (Abbott, St. Paul, MN), as previously described by Deno et al,[12] is a 4-by-4 unipolar electrode array with 1-mm (diameter) electrodes, equidistantly spaced 4 mm apart from each other. Similarly, the HD 56 (Abbott) is a 7-by-8 unipolar electrode array with 1-mm (dia) electrodes, equidistantly spaced 2 mm apart from each other. Lastly, our custom-made HD plaque (University Health Network, Toronto, ON, Canada) has an 8-by-14 unipolar electrode array, with 1.0-mm (dia) electrodes spaced equidistantly from each other by 2.4 mm.

Bipolar Voltage Mapping

Keeping interelectrode distance uniform for each electrode array, bipolar electrograms were derived from adjacent

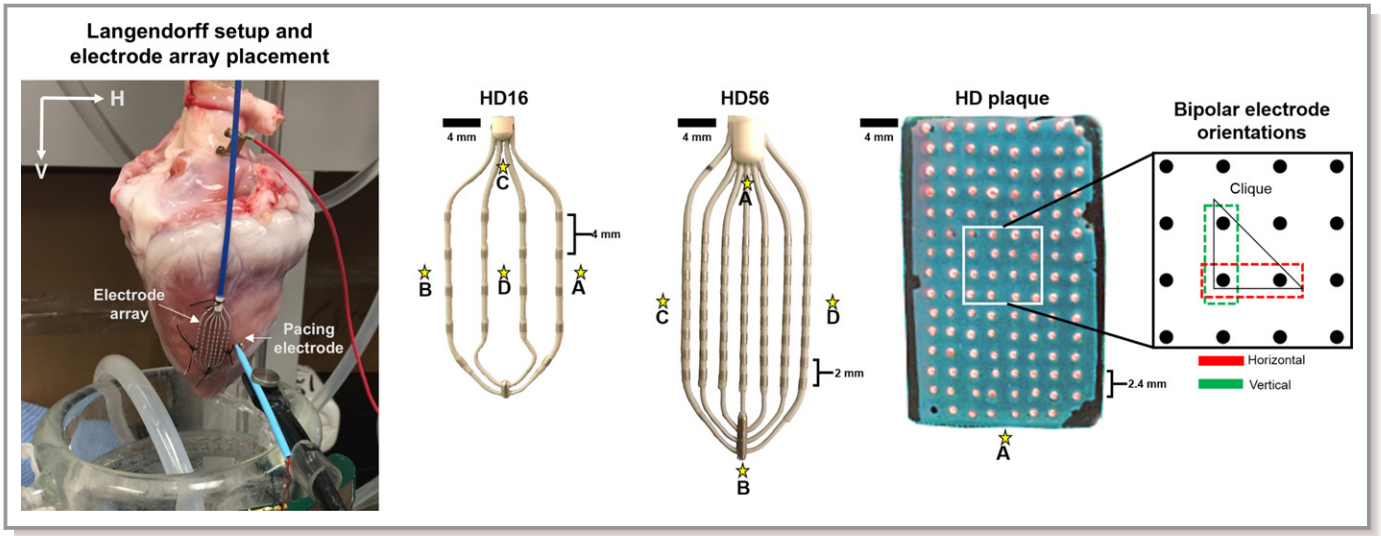

Figure 1. Langendorff setup and 2-dimensional electrode arrays: HD16, HD56, and HD plaque arrays. An experimental setup is shown to establish axes relative to the Langendorff suspension as well as the placement of electrode arrays and pacing electrodes. Two-dimensional electrode arrays laid and stitched flat onto a ventricular surface were used for electrical mapping. Stars indicate the pacing sites chosen for each electrode array. HD16 was used for rabbit hearts, HD56 for porcine hearts, and HD plaque for human hearts. By subtraction, bipolar voltage maps were created for 2 orthogonal electrode orientations (horizontal and vertical). Omnipolar electrograms were derived from a group of 4 adjacent electrodes in a triangular configuration (clique) of each electrode array.

unipolar electrodes along 2 orthogonal axes, horizontal (H) and vertical (V), where H and V are axes defined with respect to our Langendorff suspension, as shown in Figure 1. Bipolar voltage maps for each electrode orientation were created from bipolar electrogram Vpps that were located at the center of the line segment joining an electrode pair. Continuously colored voltage maps were created using a triangular-mesh-based interpolation method using Matlab (Mathworks, Natick, MA).

Omnipolar Voltage Mapping

As previously described by Deno et al, using 4 or 3 adjacent, closely spaced unipolar electrodes (a square or triangle clique, respectively) to map a myocardial surface, we are able to locally sense a TW. In this work, we used triangular cliques to derive E-fields to fully utilize the spatial capacity of our electrode arrays. A TW produces a spatial voltage gradient, or an E-field, which could be derived using OT. We can mathematically determine a TW's direction within a clique using its E-field. A TW's direction is derived by finding the orientation along which its time and spatial derivatives are maximally cross-correlated. The details of the derivation and validation of E-fields from unipolar electrograms have been described in previous works.[12,13] Here we present a simplified version of the OT algorithm.

A 2D E-field can be mathematically derived from a collection of M measured unipolar electrograms ($\varphi(t)$) of length N within a clique, where M is the number of electrodes required to form either a triangle or a square clique. In addition, we take note of the *x*- and *y*-coordinates of each unipolar electrode that signifies its location in the Cartesian plane. Since we are using triangular cliques, we obtain M=3 unipolar electrograms from 3 closely spaced electrodes. We label this set as $\boldsymbol{\varphi}(\mathbf{t}) = [\varphi_1(t), \varphi_2(t), \varphi_3(t)]$, which is an M-by-N matrix, with units of mV. Keeping interelectrode distance constant, we calculate possible bipolar electrograms ($\mathbf{d\varphi}(\mathbf{t})$) from this set of unipolar electrograms as shown below

$$\mathbf{d\varphi}(\mathbf{t}) = \begin{bmatrix} \varphi_1(t) - \varphi_2(t) \\ \varphi_2(t) - \varphi_3(t) \end{bmatrix}$$

We calculate the distances (d, in mm) between 2 neighboring electrodes from which the bipolar electrograms above were created by calculating the length of the line segment joining their *x*- and *y*-coordinates. We store these values in a distance matrix, **dX**, which is a 2-by-2 matrix as shown below

$$\mathbf{dX} = -\begin{bmatrix} 0 & d \\ d & 0 \end{bmatrix}$$

where each column contains the *x*- and *y*-coordinates of the 2 end points of the line segment, with mm for units. For a simple static setup where a grid is stitched on epicardium, we assume that electrode distances do not change over time. $\mathbf{d\varphi}(\mathbf{t})$ is then projected into clique space, **dX**, to calculate the resultant 2D E-field, $\mathbf{E}(\mathbf{t})$, which is a 2D vector such that

$$\mathbf{E}(\mathbf{t}) = \begin{bmatrix} \mathbf{E_x} \\ \mathbf{E_y} \end{bmatrix} = \mathbf{dX'd\varphi(t)}$$

Each component of $\mathbf{E}(\mathbf{t})$ has a length of N, with units of mV/mm. We then scale $\mathbf{E}(\mathbf{t})$ with the average interelectrode distance (ID, in mm) within a clique, which results in a 2D voltage vector $\vec{\mathbf{v}}(\mathbf{t})$ of length N, with units of mV, such that

$$\vec{\mathbf{v}}(\mathbf{t}) = \begin{bmatrix} \vec{\mathbf{v}}_\mathbf{x} \\ \vec{\mathbf{v}}_\mathbf{y} \end{bmatrix} = \mathbf{E}(\mathbf{t}) * \mathrm{ID}$$

$\vec{\mathbf{v}}(\mathbf{t})$ can be projected to different angles to derive bipolar-like electrograms along such angles, similar to incrementally rotating a bipolar electrode to examine all orientations. From the angle that the time and spatial derivatives of a TW are maximally cross-correlated, not only can we determine the activation direction of a wavefront but also electrode orientation–independent omnipolar electrograms, OT_{egm}, from which we can derive OT_{Vmax} that is along the maximal bipole direction. We can calculate OT_{Vmax} from $\vec{\mathbf{v}}(\mathbf{t})$ by using the following equation:

$$OT_{Vmax} = \max\left\{\left|\vec{\mathbf{v}}(t_i) - \vec{\mathbf{v}}(t_j)\right|\right\}$$

where t_i and t_j are 2 time points within the analysis interval such that length of $\vec{\mathbf{v}}(\mathbf{t})$ is the greatest. OT_{Vmax} values obtained from each triangle clique were used to create unambiguous voltage maps that reflect underlying physiology on the myocardial plane. Each OT_{Vmax} value was located at the center of each clique, which we interpolated across the entire electrode array using the same method used for bipolar voltage maps to create continuous OT_{Vmax} voltage maps. Proof of concept of this technique was recently presented by our group on rabbit and human data.[14]

Rabbit Heart Experiments

Whole hearts were harvested from 5 healthy New Zealand White male rabbits weighing between 3 and 4 kg. After explantation, a heart was placed in a cold Tyrode solution, which was then delivered to an adjacent room, less than 5 minutes away. The heart was flushed thoroughly to remove any blood particles. Each heart was cannulated through the aorta and secured with 2-0 silk sutures to the cannula. Each heart was then perfused with Tyrode solution (95% O_2, 5% CO_2), with its mean pressure and temperature maintained at 55 mm Hg and 37°C, respectively. The heart was then allowed to stabilize for about 10 minutes, after which our mapping protocol was conducted. The HD 16 was stitched epicardially on the left ventricular free wall, with the distal end of the catheter pointing towards the apex. Each heart was paced at 3 Hz at 4 different locations relative to the electrode array shown in Figure 1. Unipolar electrograms containing 10 beats, sampled at 1 kHz and filtered between 0.5 Hz and 200 Hz, were acquired using our data acquisition system (UHN Cathlab Cardiac Mapping System[15,16]). Additionally, all derived and OT computed bipolar electrograms from both electrode orientations were high-pass filtered at 35 Hz as per clinical standards. For each rabbit heart, 12 bipolar electrogram Vpp measurements for each H and V orientation were obtained and 36 OT_{Vmax} values were calculated from all triangle cliques within the HD16 grid.

Porcine Heart Experiments

Five whole hearts were harvested from healthy male Yorkshire pigs, with an average weight of 36 kg. Similar protocols for transportation, cannulation, and perfusion with rabbit hearts as described above were followed. The HD 56 was stitched epicardially on the left ventricular free wall, with the distal end of the electrode array pointing towards the apex. Each heart was paced at 4 different locations relative to the electrode array as shown in Figure 1. After mapping healthy myocardium, each porcine heart was radiofrequency ablated using a 3.5-mm clinical catheter to produce scarring in the myocardium. For both healthy and ablated myocardia, unipolar and bipolar electrograms were acquired and treated the same as with rabbit hearts. Corresponding bipolar Vpps were derived from both electrode orientations as previously described. Data from radiofrequency ablated porcine hearts were used for substrate mapping. For each porcine heart, there were 49 and 48 bipolar Vpps from H and V electrode orientations, respectively, and 168 OT_{Vmax} values calculated from all triangle cliques within HD 56 grid.

Human Heart Experiments

Five myopathic human hearts were obtained from heart transplant recipients at the time of their surgery with informed consent. We followed a similar protocol for transportation, cannulation, and perfusion with rabbit and porcine hearts as described above. The HD plaque was stitched to the left ventricular septum of each heart and electrically mapped while being paced at approximately 300 ms. Unipolar electrograms with 10 beats were acquired and filtered, similarly to rabbit and porcine hearts. Furthermore, calculated bipolar electrograms were highpass filtered at 35 Hz. There were 104 bipolar electrogram Vpps measured for H orientation, 98 bipolar electrogram Vpps measured for V orientation, and 364 OT_{Vmax} values calculated from all triangle cliques within the HD plaque.

Quantitative Analysis

To simplify electrode orientation, voltage, and beat-to-beat variability analysis of omnipole and bipole on healthy rabbit and porcine hearts and diseased human hearts, we used data obtained from a single pacing location (Figure 1, site A). Data from all 4 pacing locations, for a single beat, from rabbit and porcine hearts were used to analyze variabilities of omnipolar and bipolar voltages caused by rhythm changes. Lastly, we used data from radiofrequency-ablated porcine hearts to explore the value of omnipoles for substrate mapping by developing electrode-array-specific voltage thresholds, which we use to delineate radiofrequency lesions.

Electrode orientation analysis

To demonstrate to what degree the bipolar voltage maps are influenced by electrode orientation, we calculated mean absolute differences between H and V bipolar Vpps for all 10 beats, from all cliques within each electrode array for all rabbit, porcine, and human hearts. We tested the null hypothesis that there is no difference between the means of H bipolar Vpps and V bipolar Vpps, for each clique, for each heart.

Relationship of omnipoles with measurable bipolar electrogram with the largest Vpp

We calculated the mean absolute differences between H bipolar Vpps and V bipolar Vpps with OT_{Vmax} values, separately, to analyze whether OT_{Vmax} values, for all 10 beats within each clique, provide larger voltages than either of the bipolar Vpps. We calculated the correlation of the Vpp distribution of the largest bipoles from all 10 beats and each clique to explore the relationship of the largest measurable bipolar Vpps to OT_{Vmax} values. Furthermore, we correlated the morphologies of measured bipolar electrograms with the largest Vpps (from either H or V axis) with OT_{egms} to determine whether there is any similarity between traditional bipolar electrograms if they were approximately aligned with the maximal bipole direction.

Evaluation of beat-to-beat and rhythm variability of omnipoles and bipoles

We measured beat-to-beat voltage variability of voltage maps by coefficient of variation (t-CoV) of H and V bipolar Vpps and OT_{Vmax} values from all rabbit, porcine, and human hearts. This was calculated by taking the ratio of the standard deviation to average values of both H and V bipoles and OT_{Vmax} of all 10 beats within each clique. A CoV value of 0 indicates perfect consistency while a CoV value close to 1 indicates increasing variability. We measured rhythm variability (r-CoV) of H and V bipolar Vpps and OT_{Vmax} values within each clique only from rabbit and porcine hearts, which were paced at 4 different sites. We also calculated CoV for this portion; however, the means and standard deviations were calculated from the voltage values from each clique across the 4 resultant voltage maps (corresponding to 4 different pacing locations).

Statistical analysis

For a single pacing site, within each animal group, for all cliques, and for all beats, the differences between H and V, OT_{Vmax} and H, and OT_{Vmax} and V were analyzed using hierarchical mixed effect, and random intercept model provided the best model fit as measured using the model, accounting for nested clustering (beats within cliques within hearts) and repeated measures per subject. After running linear regression, marginal predictions were used to perform the pairwise comparisons of OT_{Vmax} values and H and V bipolar Vpps. Statistical analysis was performed using Stata Version 12.

A standard paired *t* test was used for the statistical analysis of the distribution of t-CoV values (within 10 beats) and r-CoV values (for 4 pacing sites) between bipoles and omnipoles obtained from each clique from each animal. Graphpad Prism 6 was used for this analysis.

For both statistical tests, we used a *P* value cutoff of 0.05 (P=0.05) with which we determine statistical significance. Any tests that yield *P* values lower than 0.05 were determined to be statistically significant (S), while $P \geq 0.05$ were determined to be nonstatistically significant.

Determining Dense Scar Voltage Threshold for Omnipolar Voltage Maps

To determine an appropriate OT_{Vmax} threshold value measured from the 2-mm HD56 grid, a blind study was performed with 3 electrophysiologists who were tasked to determine the status of the epicardium within each triangular area, delineated by 3 closely spaced electrodes, for each of the radiofrequency-ablated porcine hearts. The electrophysiologists identified whether the area is scarred, a border zone, or normal tissue by visual inspection. For a particular area of the myocardium underneath the grid to be identified as scarred, border zone, or normal, all 3 electrophysiologists must unanimously agree on its condition. Subsequently, the values of previously calculated OT_{Vmax} from classified zones were pooled from all porcine subjects. Similar to our previous work,[17] to compare scar profiles created from bipolar and OT_{Vmax} voltages, we used 2 voltage thresholds; first, the traditional bipolar voltage threshold for dense scar ($\leq$0.5 mV); second, the catheter-specific OT_{Vmax} value threshold for dense scar as measured from an HD56. We then quantified

the scar areas (in mm^2) relative to the mapping area of HD56 grid for both bipolar and omnipolar voltage maps for each voltage threshold used. We validated our area measurements by calculating the actual area of lesions from a sample lesion photograph through an open-source image processing software (GIMP 2).

Results

Electrode Orientation Affects Overall Bipolar Voltage Map Profiles

We demonstrated that the voltage maps derived from both H and V bipolar electrode orientations measure distinct electrograms, and therefore provide unique Vpps. As shown in Figure 2, this translates to differing bipolar voltage map profiles for the same substrate. For example, in Figure 2A, the V bipole measured only 4.00 mV while the H bipole measured 5.45 mV. Figure 3A shows, for a single pacing location, for all 10 beats, and for all cliques from each electrode array within each species, that although the absolute value of the differences between all the paired H and V bipolar Vpp values did not reach statistical significance according to our hierarchical mixed effect model ($\alpha<0.05$, 0.17 ± 0.18 mV, 0.43 ± 0.24 mV, and 0.25 ± 0.18 mV for rabbit, porcine, and humans, respectively), the difference between resultant color maps from individual electrode orientations clearly shows the influence of electrode orientation to bipolar voltage mapping as indicated by the wide range of colors represented within each map.

Omnipoles Provide the Largest Possible Bipolar Voltages

We demonstrated that omnipoles provide bipolar Vpps that are larger than any of the measured bipolar Vpps from the 2 electrode orientations. As shown in Figure 2, in the bottom panels, the OT_{Vmax} voltage maps from healthy rabbit (Figure 2A) and porcine (Figure 2B) myocardium $\geq$5.0 mV, were predominantly colored with dark blue, while the OT_{Vmax} voltage map from a diseased human heart (Figure 2C) shows a combination of areas with the largest Vpps from both H and V bipolar voltage maps. In a healthy rabbit heart shown in Figure 2A, we calculated an OT_{Vmax} value of 7.5 mV, which is 3.5 mV and 2.0 mV larger than the measured V and H bipolar Vpps, respectively, within the same area. For a single pacing site, for all 10 beats, and for all cliques for each electrode array within each species, the mean absolute differences between OT_{Vmax} and V Vpp distributions are 1.66 ± 0.18 mV, 2.17 ± 0.24 mV, and 1.35 ± 0.18 mV for rabbits, porcine, and

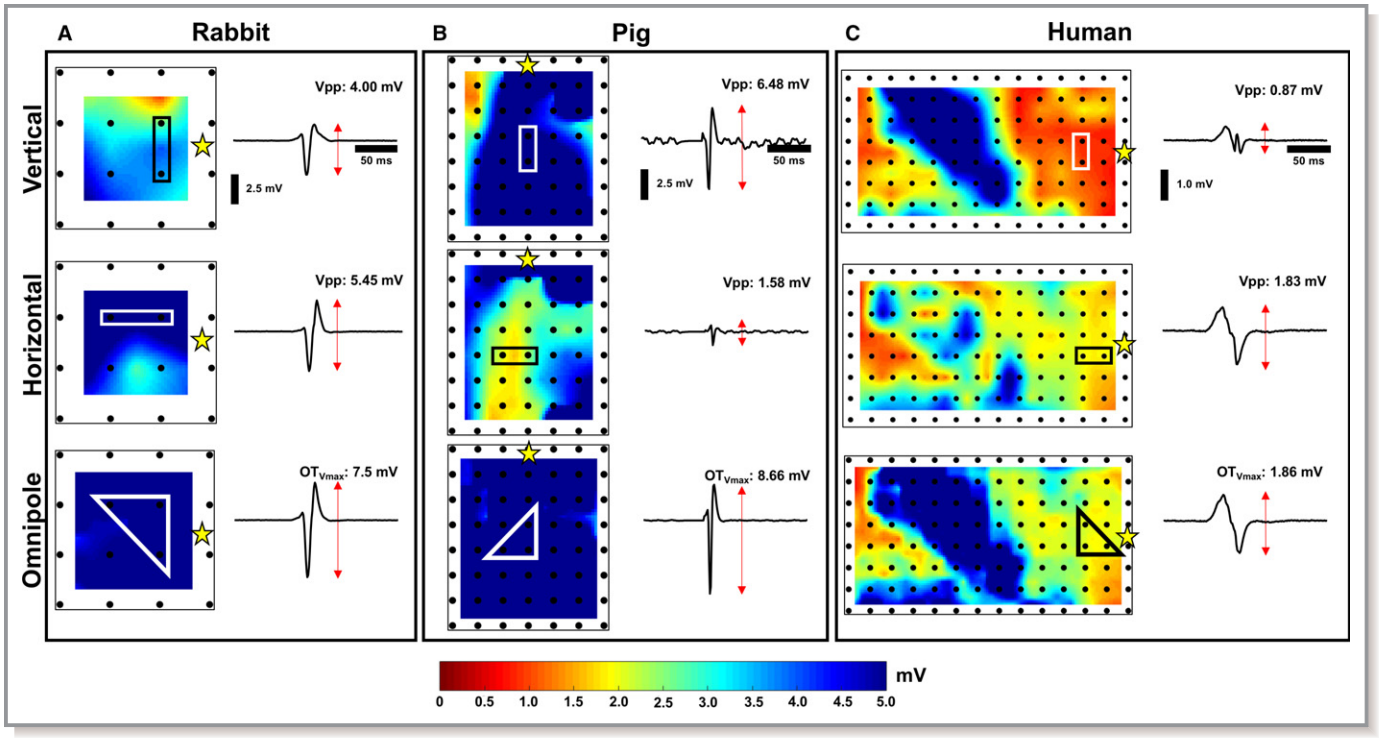

Figure 2. Bipolar and omnipolar voltage maps. For a single pacing (yellow star) location, bipolar electrograms and voltage maps derived from data collected from 3 arrays from a rabbit heart (A), porcine heart (B), and human heart (C), as shown in the top and middle panels, depict evidence of the bipolar electrogram's dependence on electrode orientation. In contrast, a maximal bipolar electrogram, OT_{egm}, could provide the maximal bipolar voltage, OT_{Vmax}, within an area and be used to create unambiguous voltage maps. Vpp indicates voltage peak-to-peak.

humans, respectively; the mean absolute differences between OT_{Vmax} and H Vpp distributions are 1.49±0.18 mV, 2.61±0.24 mV, and 1.60±0.18 mV for rabbits, porcine, and humans, respectively. All comparisons were found to be statistically significant through our hierarchical mixed effect model (α<0.05), all of which are outlined in Figure 3B. This is further supported in Figure 4A where OT_{Vmax} values are always equal to or larger than the measured bipole with the largest Vpp, regardless of electrode orientation, as the majority of points in the scatter plot are above or equal to the line of unity shown as a red line.

OT_{egms} and OT_{Vmax} Are Highly Correlated With Measured Bipolar Electrograms With Largest Vpps

We demonstrated here that OT_{egms} and OT_{Vmax} are similar to both morphology and Vpp of a measured bipolar electrogram that has the largest Vpp and that is approximately aligned in the maximal bipole direction. As shown in Figure 3C, for a single pacing location, for all 10 beats, for all cliques for each electrode array for each species, we calculated the correlation coefficient of the distribution of OT_{Vmax} values and the largest measured bipolar Vpps, from either H or V bipolar orientation, and found that they are highly correlated to each other with 0.95±0.01, 0.97±0.03, and 0.97±0.08 for rabbits, porcine, and humans, respectively. We illustrate this relationship in Figure 4A for each of species where the OT_{Vmax} values are greater than (up to 5.0 mV) or equal to the measured bipolar electrogram with the largest Vpp, from either H or V electrode orientation.

Furthermore, we examined the similarity of morphologies between the OT_{egm}s and bipolar electrograms with the largest Vpp. For a single pacing site, for all 10 beats, and for all cliques within the electrode array for each species, we calculated the correlation coefficients between these electrograms and found that they are correlated by 0.94±0.10, 0.94±0.08, and 0.94±0.08 for rabbits, porcine, and humans,

Summary of Measurements and Comparison – Bipole vs. Omnipole

	Rabbit (n = 5)	**Porcine** (n = 5)	**Human** (n = 5)
A) Vpp – Bipoles			
V (avg ± std) mV	4.23 ± 1.94	4.09 ± 2.13	3.80 ± 5.56
H (avg ± std) mV	4.40 ± 1.13	3.52 ± 2.11	3.56 ± 4.93
Δ |H – V| mV, p (HME)	0.17 ± 0.18, **NS**	0.43 ± 0.24, **NS**	0.25 ± 0.18, **NS**
B) Vpp – Omnipole			
OT_{Vmax} (avg ± std) mV	5.89 ± 1.19	6.23 ± 6.90	5.17 ± 6.96
Δ |OT_{Vmax} – V| mV, p (HME)	1.66 ± 0.18, **S**	2.17 ± 0.24, **S**	1.35 ± 0.18, **S**
Δ |OT_{Vmax} – H| mV, p (HME)	1.49 ± 0.18, **S**	2.61 ± 0.24, **S**	1.60 ± 0.18, **S**
C) Correlations (r) – OT_{Vmax} vs. Maximal (H or V) Bipole Vpp			
Vpp (avg ± std)	0.95 ± 0.01	0.97 ± 0.03	0.97 ± 0.08
Morphology (avg ± std)	0.94 ± 0.10	0.94 ± 0.08	0.94 ± 0.08
D) Beat-by-Beat Variation (t-CoV)			
Bipole (avg ± std)	0.27 ± 0.19	0.33 ± 0.21	0.28 ± 0.19
OT_{max} (avg ± std)	0.01 ± 0.02	0.09 ± 0.11	0.08 ± 0.13
p-value, (paired t-test)	p < 0.01	p < 0.01	p < 0.01
E) Rhythm Variation (r-CoV)			
Bipole (avg ± std)	0.43 ± 0.23	0.55 ± 0.21	N/A
OT_{max} (avg ± std)	0.29 ± 0.23	0.40 ± 0.20	N/A
p-value, (paired t-test)	p < 0.01	p < 0.01	N/A

Figure 3. Summary of quantitative analysis performed to compare omnipolar and bipolar measurements. With a *P* value cutoff of 0.05 to determine statistical significance, NS (nonsignificant) indicates $P \geq 0.05$, while an S (significant) indicates $P<0.05$ for both our hierarchical mixed effect (HME) model and standard paired *t* test. r-CoV indicates rhythm variability; t-CoV, temporal variability, ; Vpp, voltage peak-to-peak.

respectively, which are shown in Figure 3C. Examples of these are shown in Figure 4B. These similarities are very well shown with the electrograms from diseased human hearts where the bipolar electrogram from the H axis is similar in both morphology and Vpp to OT_{egm} for a particular area highlighted in Figure 2C. We summarize the relationships between the omnipoles and measurable bipoles with the largest Vpps on bar plots shown in Figure 4C.

Omnipoles Provide Better Beat-to-Beat Voltage Consistency Than Traditional Bipoles

For a single pacing location, we examined beat-to-beat variability (t-CoV) of voltage maps created from bipolar Vpps against those created from OT_{Vmax} by examining beat-by-beat CoVs from all rabbit, porcine, and human heart ventricles. As outlined in Figure 3D and shown in Figure 5A, the mean t-CoV of bipolar Vpps across all rabbit hearts were calculated to be 0.27±0.19 while the t-CoV for OT_{Vmax} values were only 0.01±0.02 (P<0.01). In addition, 0.33±0.21 is the mean t-CoV of bipolar Vpps across all porcine hearts while OT_{Vmax} values only have mean t-CoV of 0.09±0.11 (P<0.01). Lastly, in all human hearts, omnipoles are more temporally consistent than bipoles, with bipolar Vpps mean t-CoV at 0.28±0.19 while OT_{Vmax} values at 0.08±0.13 (P<0.01).

Omnipoles Provide Better Rhythm Consistency Than Traditional Bipoles

For a single beat, we examined rhythm variability (r-CoV) of voltage maps created from bipolar Vpps against those created from OT_{Vmax} across 4 different pacing sites in all rabbit and porcine hearts. As outlined in Figure 3E and as shown in Figure 5B, the mean r-CoV of bipolar Vpps across all rabbit hearts was calculated to be 0.43±0.23 while the r-CoV for OT_{Vmax} values were only at 0.29±0.23 (P<0.01). In addition, 0.55±0.21 is the mean r-CoV of bipolar Vpps across all porcine hearts while OT_{Vmax} values only have 0.40±0.20 (P<0.01). A visual representation of this protocol can be seen in Figure 6.

Omnipolar Voltage Mapping: An Alternative to Traditional Bipolar Voltage Mapping

As a result of the blinded study, we pooled all the OT_{Vmax} values from each clique that were classified as voltages that correspond to scar, scar border, and healthy tissues with

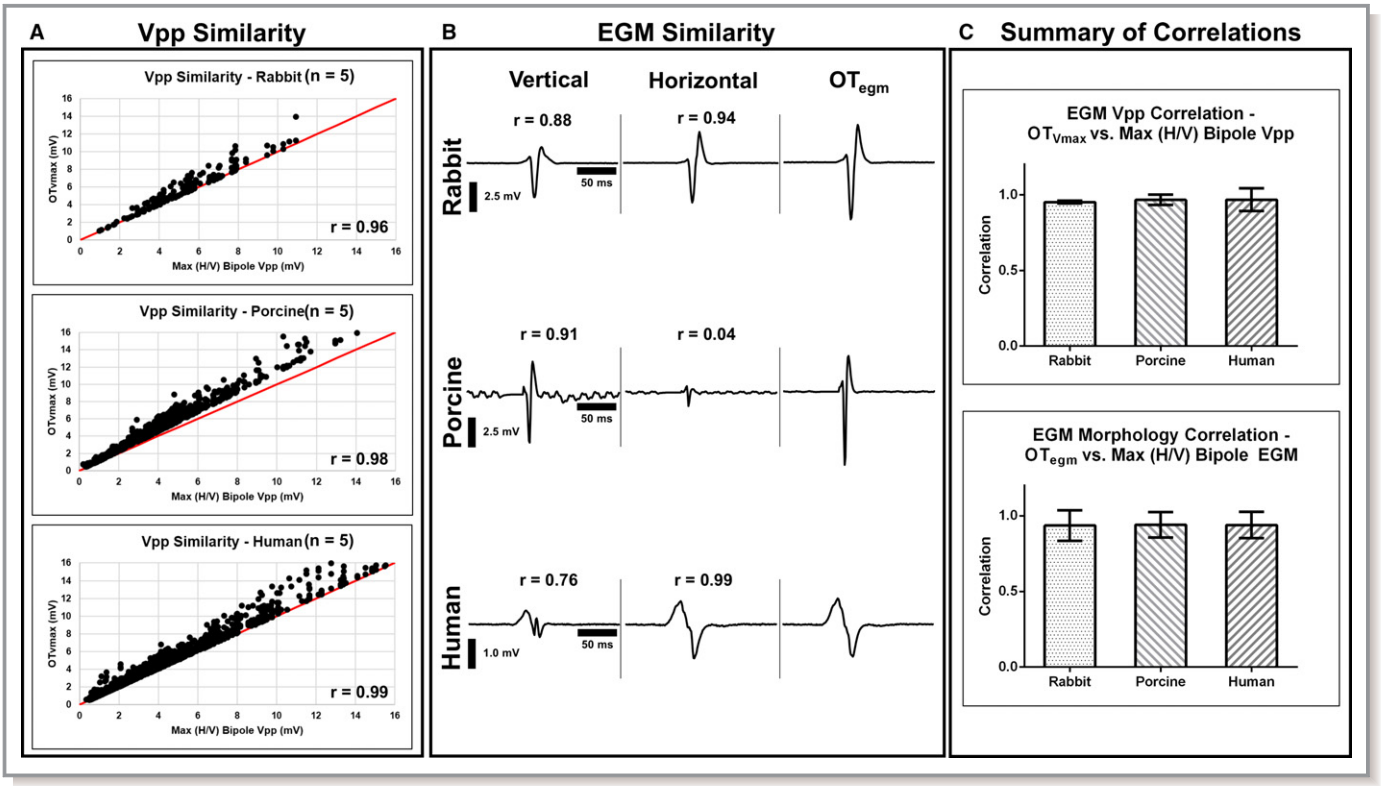

Figure 4. Validation of OT_{Vmax} and OT_{egm}. We validated our claim that OT calculates voltages along the maximal bipole direction, which is similar to a traditional bipolar electrogram (EGM) if it were manually measured along this direction. For all subjects, each clique, and for all 10 beats, we found that bipolar EGMs with the largest Vpps, from either H (horizontal) or V (vertical) orientation, are greatly correlated with OT_{Vmax} and OT_{egm} in terms of their Vpp distributions (A) and EGM morphology (B). We show correlations summary on (C). OT_{egm} indicates maximal bipolar electrogram; OT_{Vmax}, omnipolar-derived measurements of peak-to-peak voltage; Vpp, voltage peak-to-peak.

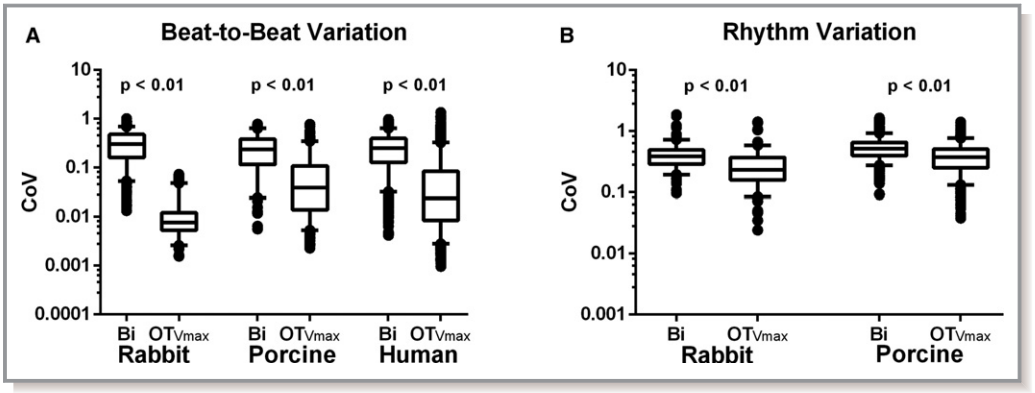

Figure 5. OT_{Vmax} is less variable, throughout multiple beats and rhythms compared to traditional bipolar voltage peak-to-peak. Using coefficients of variation (t-CoV) over 10 beats for all subjects, we demonstrated that OT_{Vmax} is less variable beat-to-beat compared with bipolar Vpps indicated by its significantly low mean t-CoV values (A). On the other hand, rhythm CoV (r-CoV) of OT_{Vmax} over 4 pacing sites is, overall, a magnitude higher than its t-CoV; however, it is still less than the r-CoV of bipoles (B). The rhythm variations of bipolar Vpps could be influenced not only by anatomy and/or physiology of the myocardium but also by electrode orientation, whereas the rhythm variations of OT_{Vmax} may be a reflection of only tissue characteristics. OT_{Vmax} indicates omnipolar-derived measurements of peak-to-peak voltage; r-CoV, temporal variability; Vpps, voltage peak-to-peak.

respect to their location on the radiofrequency-ablated myocardium as mapped by the HD56. As shown in Figure 7A, normal distributions were modeled from the mean (μ) and standard deviations (σ) of the OT_{Vmax} histograms of pooled scar and scar border voltages. Rounded up to the nearest tenths, the OT_{Vmax} threshold value for both scar and scar border were chosen to be $\mu+1\sigma$. The OT_{Vmax} threshold values for scar and scar borders were found to be 1.5 mV and 2.0 mV, respectively.

Furthermore, we created a receiver operating characteristic curve to evaluate the sensitivity and specificity of the derived OT_{Vmax} threshold value for scar. Shown in Figure 7B is the receiver operating characteristic curve plotted with a unity line for reference. At the 1.5-mV cutoff, the true positive rate was as high as 0.94 while the false positive rate was only 0.18. In contrast, the conventional threshold (<0.5 mV), true positive rate, and false positive rate values are only 0.078 and 0, respectively.

As reference, we calculated the perceived scar area on the radiofrequency-ablated myocardium of porcine #2 as shown in Figure 8 through an image processing software. The area was calculated to be 20.0 mm^2. Shown in Figure 7C, using the catheter-specific voltage threshold ($\leq$1.5 mV) for OT_{Vmax}, a 17.0 mm^2 of scar area was detected, which is closer to the calculated reference compared with those areas that were detected by H and V bipolar voltage maps in this catheter-specific voltage threshold, 52.3 mm^2 and 25.0 mm^2, respectively.

Using the traditional bipolar Vpp threshold of <0.5 mV for myocardial scars, we show on the middle panel of Figure 8 that 2 orthogonal bipolar electrodes provide different lesion profiles for radiofrequency-ablated porcine hearts, simulating a lesion gap. The voltage map created with bipolar Vpp values along the V direction provide approximate locations of the 2 radiofrequency ablation lesions on the epicardium; however, the lesion on the right side of the grid is smaller than its actual size. Most of the right-side lesion is labeled as scar border instead. The representation of the right-side radiofrequency lesion was drastically changed with the bipolar Vpp values along the H direction because there is virtually no myocardial scar at that area while the boundaries of the left-side radiofrequency lesion have been dramatically changed. On the other hand, we illustrate the application of the newly determined low-voltage scar area threshold for OT_{Vmax} in Figure 8. Using $\leq$1.5 mV as a threshold, the lesions on both sides of the grid are better defined, hence a lesion gap could be seen clearly on the omnipolar voltage map, which has been visually verified. Using the same threshold on bipolar voltage maps, we found that the areas of radiofrequency lesions were overestimated by 19$\pm$15% and only on the map where the bipoles are aligned along the V-axis was a lesion gap observed.

Discussion

We have demonstrated in this article that traditional bipolar voltage maps could vary significantly depending on electrode orientation and thus provide unreliable representation of the of the myocardium. As a potential solution, we introduced omnipolar voltage maps that are derived from electrograms along the maximal bipolar direction at any given site. Furthermore, omnipoles are consistent within beats and with different rhythms compared to traditional bipoles. If this novel strategy can be

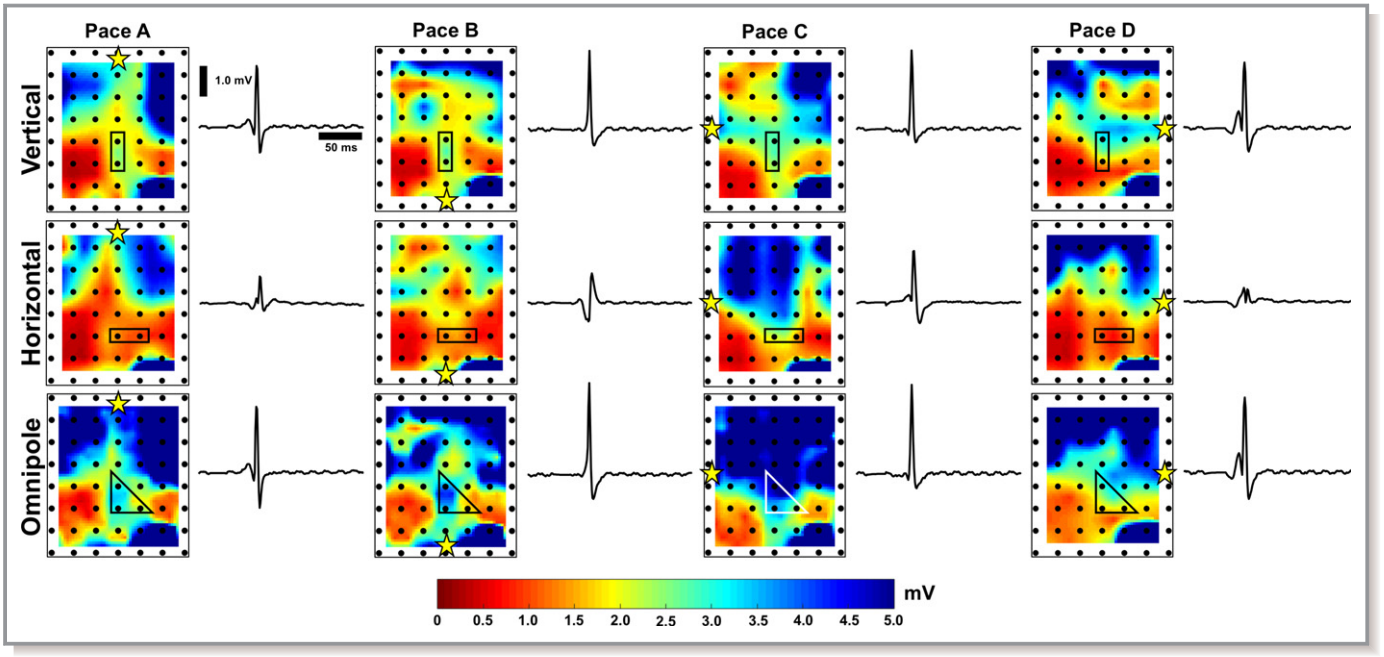

Figure 6. Voltage map variability as a reflection of local tissue characteristics. For 2 orthogonal bipolar electrode orientations, 8 unique voltage maps and sample electrograms were generated (under paced condition with a yellow star indicating pacing location), which could signify voltage variability caused by both tissue characteristics as well as electrode orientation. By using omnipoles, we greatly narrow down voltage map variability as demonstrated by 4 unique voltage maps, which correspond to 4 pacing locations indicated by yellow stars in each map. This could be a reflection of physiological or structural tissue properties, which could be important in substrate characterization. Furthermore, there is better delineation of myocardial scars within omnipolar voltage maps, whereas scar profiles within bipolar voltage maps could greatly vary.

successfully implemented in 3D mapping systems, this could translate into a real-time solution for the ambiguous bipolar voltage maps and misleading interpretation of the underlying physiology of the myocardial substrate in question. This could advance delineation of possible targets for ventricular tachycardia ablation therapy once prospectively tested.

Omnipoles Provide Voltages Along the Maximal Bipole Direction

We previously demonstrated that bipolar voltage profiles could change depending on the orientation of electrodes and that electrode-orientation independent omnipoles could be used to provide unambiguous electrograms with the largest

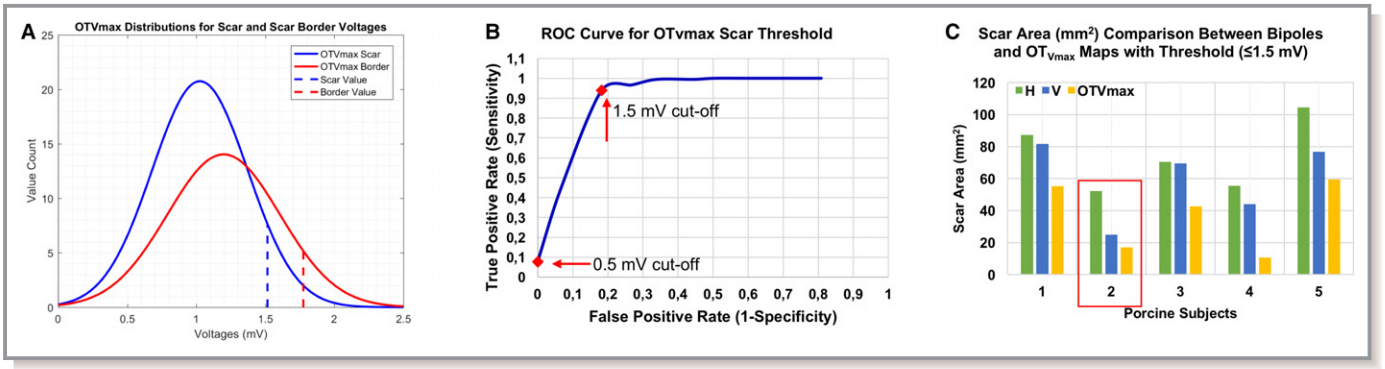

Figure 7. OT_{Vmax} voltage threshold better delineates scarred areas than bipoles. (A) All the OT_{Vmax} values that were classified as voltages from scar and scar border areas were pooled from our blinded study. Normal distributions for both groups were modeled after their mean (μ) and standard deviations (σ). Voltage thresholds were chosen to be μ+1σ (B) with the determination of voltage threshold for OT_{Vmax}, an ROC curve was created from which we found that OT_{Vmax} threshold value is sensitive and specific to scars created from radiofrequency ablation. With a reference area of 20.0 mm^2 from porcine #2 (highlighted in red box) (C) with the use of catheter-specific voltage threshold (≤1.5 mV), OT_{Vmax} voltage map detected scar with an area of 17.0 mm^2, which is closer to the reference area, while bipolar voltage maps tend to overestimate such areas (52.3 mm^2 for H [horizontal] and 25.0 mm^2 for V [vertical]). OT_{Vmax} indicates omnipolar-derived measurements of peak-to-peak voltage; ROC, receiver operating characteristic.

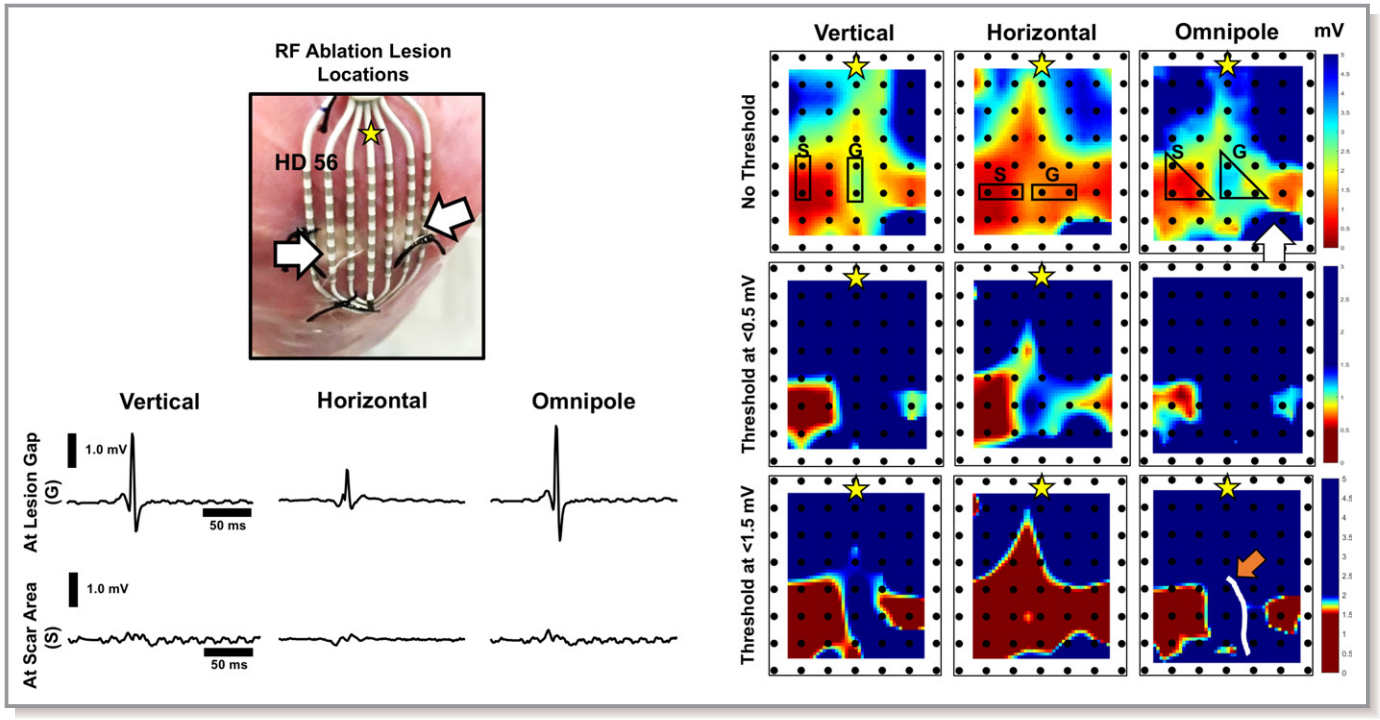

Figure 8. Incremental value of omnipoles in substrate mapping. With empirically determined OT_{Vmax} threshold (<1.5 mV) based on its values at the locations of RF lesions from all porcine hearts, the incremental value of omnipoles as a tool for substrate mapping becomes evident. Lesion gap and/or isthmus detection could be 1 particular example of an application of omnipoles for substrate mapping (orange arrow). When compared with voltage maps that use the traditional dense scar bipolar Vpp threshold (< 0.5 mV), RF lesions are scarcely delineated, much less the lesion gap. Accompanying electrograms at the gap (G) and on the scar (S) are shown to validate the status of the tissue. A visual comparison, overlaid with a representation of the HD56, shows that there is indeed a gap that exists between the 2 lesions that would have only been detected with bipoles if a catheter is oriented vertical to the pacing site. Yellow star indicates pacing location. Note a defective channel on the bottom right corner of each map shown by a white arrow. OT_{Vmax} indicates omnipolar-derived measurements of peak-to-peak voltage; RF, radiofrequency; VPP, voltage peak-to-peak.

Vpp that are along the maximal bipolar direction[14]. In this body of work, we have expanded our validation efforts using human and porcine data, both in healthy and in ablated myocardium, from a 2-mm HD56 2D electrode array. We quantified the advantage of omnipoles during rhythm variability and in terms of consistency for substrate mapping to extract its potential application to the clinical arena.

Omnipoles consistently provided electrograms that have the largest Vpp independent of electrode orientation, which is essential in standardizing the method of bipolar voltage mapping. Since we expected that a bipolar electrogram with the largest Vpp is attainable only if the electrodes are aligned along the maximal bipole direction, the similarity of omnipoles to these measured bipoles, in both morphology and Vpp distributions, provides confidence that the concept of omnipoles is strongly anchored on physiological foundations rather than on arbitrary positioning or grouping of electrodes. Our experiments and potential solutions are timely given the fact that Sacher and Field emphasized in their recent editorial[18] the problem defined by Tung et al[19] on the critical relationship between wavefront direction and voltage maps. They called for the need to better understand the variables that influence generation of bipolar voltage maps, 1 of which is electrode orientation; as such, our work provides 1 potential solution to this dilemma. Anter and Josephson[6] previously alluded to this important concept that a biopolar electrogram oriented along the activation direction has the largest Vpp.

Our statistical findings from our hierarchical mixed effect model for paired orthogonal bipolar electrograms, comparing their absolute differences, are noteworthy. As we have cited in our results, although their voltage map profiles are strikingly different from each other, we did not find their absolute differences to be statistically significant. Even if 1 or more results have yielded statistical significance, because of multiple hypothesis tests, this may be because of chance alone. In our experiments, we used a point-source pacing electrode, which then made a point-source wave propagation instead of a uniform wave propagation throughout the span of the 2D grids. Instead of waves traveling perfectly along a bipole axis, our pacing method has created waves with great curvatures. Coupled with tissue anisotropy, this created a

random effect in our statistics such that at some areas of the grid, bipolar electrograms along the V-axis has larger Vpp values compared with other areas of the grid. This occurrence was also observed with bipolar electrograms along the H-axis. The range of colors presented in each of the bipolar voltage maps shown Figure 2B perfectly illustrates this concept.

OT_{Vmax}, despite wave curvatures, was able to detect the electrogram that has the largest Vpp value as if a bipolar electrode was adjusted to be aligned along these curves, hence producing a more uniform voltage map as shown with relatively narrow range of colors at the bottom panel of Figure 2B.

Omnipoles Offer Voltages With Greater Beat-to-Beat Consistency

In addition to the fact that omnipoles provide physiological assessment of voltage, they are also consistent on a beat-by-beat basis compared with traditional bipoles. This means that for every beat within the same mapping area, bipoles can still have widely varying morphologies, and hence Vpps, as dictated by its electrode orientation. With regard to the issue of constructing time-consistent voltage maps, omnipolar voltage assessment could prove useful, especially when surveying hard-to-reach areas within the endocardium where an electrophysiologist is required to constantly change the orientation of his/her mapping catheter. OT_{Vmax} ensures that the largest bipolar Vpp within that area will always be obtained as opposed to Vpps from traditional bipoles because there is no guarantee that bipolar electrodes will always land on the myocardium the exact same way during the mapping procedure.

Omnipoles Offer Voltages With Greater Consistency Relative to Rhythm Changes

Voltage maps created from omnipoles also remain relatively more consistent with changes in rhythm compared with traditional bipoles. Observed inconsistencies from traditional bipoles are in accordance with the results that have been previously shown by Tung et al in their patient studies regarding changes observed in bipolar voltage map profiles relative to the change in pacing sites.[19] We postulate that the variabilities that we see in bipoles are not only caused by electrode orientation but also are coupled with variations in local tissue properties. On the contrary, since omnipoles are electrode orientation independent, variabilities relative to rhythm changes observed with omnipoles could represent important substrate characteristics that could be obscured by variabilities originating from electrode orientation. For example, variabilities seen on omnipolar voltage maps could indicate electrical anisotropy within the myocardium as a result of structural discontinuities. This tissue property was previously shown by Caldwell et al from 3D transmural activation mapping of porcine hearts.[20] Structural characteristics of myocardial tissues could affect the spread of activation depending on the wave origin, which confirms the above observations made by Tung et al. Without the influence of electrode orientation, omnipoles could be a better tool than bipoles in creating more physiologically and/or structurally meaningful voltage maps.

Potential Use of Omnipoles for Accurate Myocardial Characterization

Anter and Josephson have illustrated the pitfalls of bipolar substrate mapping. Important among those is the common belief that low bipolar voltage amplitude (<0.5 mV) implies the existence of dense scar over mapping areas. On the contrary, Soejima et al[21] have shown that there might still be surviving excitable tissue within these areas that are important for a ventricular tachycardia circuit that has been verified using a high-resolution electroanatomic mapping system.[8] Above, we have shown that bipolar voltages could greatly vary depending on electrode orientation and wavefront direction; hence, bipolar voltages do not necessarily represent the characteristics of a substrate. This property of bipoles creates ambiguity, especially when we attempt to identify or delineate low-voltage areas within the myocardium. Furthermore, Tung et al illustrated that in actual myocardial scars, variations in activation directions are exacerbated.[22] This could further affect delineation of such areas using bipolar voltages as we have shown as they are susceptible to rhythm changes.

The current “gold standard” for bipolar voltage threshold for identifying low-voltage, diseased areas is <1.5 mV, with <0.5 mV for dense scar[1,23]; however, the value of this threshold has now come into question given the factors that affect the reliability of bipolar voltages. For example, Gianni and Natale also questioned the appropriateness of application of fixed bipolar voltage thresholds to different catheter designs and substrates.[24] It was also recommended from Tung et al’s work on bipolar thresholds that such values must be constantly adapted depending on the instruments used for mapping.[22] Hence, we sought to adapt our voltage threshold relative to our mapping instruments and methods. With our blinded study, OT_{Vmax} values for a 2-mm HD56 grid associated with dense scar areas were determined to be 3 times larger than the current “gold standard.”

Because of the nature of OT_{Vmax}, this is an expected result as we have shown that OT_{Vmax} consistently provide larger values compared with any bipolar Vpps within the mapping area. As such, application of conventional bipolar Vpp threshold to OT_{Vmax} maps did not show any lesions. Similar to bipolar voltage maps, such lesions were severely

underestimated using the same voltage threshold. By adapting the voltage thresholds relative to the sensing catheter, in this case the HD56 grid, we obtain OT_{Vmax} voltage maps that are more representative of reality. As Tung et al showed, voltage thresholds have to be adapted to specific electrode arrays to accurately delineate areas of interest. The OT algorithm allows for such adaptation because the 2D E-field, with units in mV/mm, can be scaled to mV using the interelectrode distances within the electrode array as we have shown previously. By using this new threshold, we showed in Figure 8 that omnipoles are better in delineating radiofrequency lesions compared with traditional bipoles, which could misrepresent such areas.

By using electrode orientation independent omnipoles, it is possible to obtain maximal bipole measurements that are more physiologically representative of a myocardial substrate. Variabilities in omnipolar measurements will then be attributable only to tissue properties instead of being coupled with electrode orientation. This is especially important when mapping low-voltage areas such as dense myocardial scars. We discussed such an example of our radiofrequency-ablated porcine hearts in which 2 orthogonal bipoles provide significantly differing myocardial scar profiles for a single pacing site. With the addition of 3 other pacing sites, we have demonstrated that the variability of myocardial profiles becomes even greater. However, we demonstrated that maps generated with omnipoles have less myocardial physiological variation. This could lead to consistent and physiological delineation of myocardium in planning ablation strategies for treating ventricular tachycardias.

Limitations

The principles described in the Methods section, for explanation purposes, deal with a single planar wavefront. Often in diseased tissue, a wavefront even within a small area such as a square clique tends to be nonplanar. If we were to use a square clique, which has a large area, in certain mapping points, only a single vector and voltage would be described and will not capture complexities within the square. To deal with this limitation, we used 4 triangular cliques within each square clique to capture finer details within a smaller mapping area. This captures some of the complexities within the region and provides higher mapping resolution compared with a single omnipolar mapping point. Though the assumptions described in the Methods section regarding these concepts were simplified for a planar wave in healthy ventricle, we provide assessment of our method in diseased human hearts and radiofrequency-ablated porcine hearts to critically test the effect of irregular activation within the myocardium in a controlled fashion.

We have not dealt with propagation of wavefronts at different strata within the myocardial wall and are not aware of any other techniques that assess such conduction using endocardial bipolar electrograms to compare with our omnipolar electrograms. This article strictly deals with omnipolar projections within the plane of the myocardium and does not address voltages perpendicular/across the myocardium. The evaluation of the omnipole in the perpendicular/normal projection is beyond the scope of this article but will be a subject of a future study.

It is important that the readers recognize that the amplitude of the omnipolar electrogram does not clear the region evaluated to be nonpathogenic. This is not only true of an anatomic isthmus where the voltage is higher than the surrounding myocardial tissues, where clearly the isthmus is of significance; it is also important to recognize that voltage is only 1 aspect of myocardial physiology. Histologic correlation was not sought for this study, as the concept evaluated focused exclusively on orientation dependence of bipolar voltages.

No normal human hearts were studied because of ethical constraints, but normal animal hearts and crucial diseased human hearts were used in the validation.

Conclusions

Contemporary bipolar voltage maps are limited by their dependence on electrode orientation. Omnipolar voltages offer electrode-orientation-independent, physiologically based assessment of the myocardium by providing voltages on the plane of the myocardium along the maximal bipolar direction, which could be used for consistent physiological myocardial characterization. Prospective clinical studies are required to determine the likely therapeutic impact of this paradigm.

Sources of Funding

This study was funded by Abbott (formerly St. Jude Medical), St. Paul, MN.

Disclosures

At the time this article was written, Dr Nanthakumar and Mr Massé are research consultants for Abbott. Dr Deno is an employee of Abbott. The remaining authors have no disclosures to report.

References

1. Marchlinski FE, Callans DJ, Gottlieb CD, Zado E. Linear ablation lesions for control of unmappable ventricular tachycardia in patients with ischemic and nonischemic cardiomyopathy. *Circulation*. 2000;101:1288–1296.

2. Tschabrunn CM, Roujol S, Nezafat R, Faulkner-Jones B, Buxton AE, Josephson ME, Anter E. A swine model of infarct-related reentrant ventricular tachycardia: electroanatomic, magnetic resonance, and histopathological characterization. *Heart Rhythm*. 2016;13:273.
3. Oduneye SO, Oduneye SO, Pop M, Biswas L, Ghate S, Flor R, Ramanan V, Wright GA. Postinfarction ventricular tachycardia substrate characterization: a comparison between late enhancement magnetic resonance imaging and voltage mapping using an MR-guided electrophysiology system. *IEEE Trans Biomed Eng*. 2013;60:2442–2449.
4. Tilz RR, Makimoto H, Rillig A, Deiss S, Wissner E, Ouyang F. Electrical isolation of a substrate after myocardial infarction: a novel ablation strategy for unmappable ventricular tachycardias – feasibility and clinical outcome. *Europace*. 2014;16:1040–1052.
5. Tian J, Jeudy J, Smith MF, Jimenez A, Yin X, Bruce PA, Saba M. Three-dimensional contrast enhanced multidetector CT for anatomic, dynamic, and perfusion characterization of abnormal myocardium to guide ventricular tachycardia ablations. *Circ Arrhythm Electrophysiol*. 2010;3:496–504.
6. Josephson ME, Anter E. Substrate mapping for ventricular tachycardia: assumptions and misconceptions. *JACC Clin Electrophysiol*. 2015;1:341–352.
7. Anter E, Josephson ME. Bipolar voltage amplitude: what does it really mean? *Heart Rhythm*. 2016;13:326–327.
8. Tschabrunn CM, Roujol S, Dorman N, Nezafat R, Josephson ME, Anter E. High resolution mapping of ventricular scar: comparison between single and multielectrode catheters. *Circ Arrhythm Electrophysiol*. 2016;9:e003841.
9. Anter E, Tschabrunn CM, Josephson ME. High resolution mapping of scar-related atrial arrhythmias using smaller electrodes with closer interelectrode spacing. *Circ Arrhythm Electrophysiol*. 2015;8:537–545. DOI: 10.1161/CIRCEP.114.002737.
10. Stevenson WG, Soejima K. Recording techniques for clinical electrophysiology. *J Cardiovasc Electrophysiol*. 2005;16:1–6.
11. De Groot NM, Schalij MJ, Zeppenfeld K, Blom NA, Van der Velde ET, Van der Wall EE. Voltage and activation mapping: how the recording technique affects the outcome of catheter ablation procedures in patients with congenital heart disease. *Circulation*. 2003;108:2099–2106.
12. Deno DC, Balachandran R, Morgan D, Ahmad F, Massé S, Nanthakumar K. Orientation independent catheter-based characterization of myocardial activation. *IEEE Trans Biomed Eng*. 2017;64:1067–1077.
13. Massé S, Magtibay K, Jackson N, Asta J, Kusha M, Zhang B, Balachandran R, Radisic M, Deno DC, Nanthakumar K. Resolving myocardial activation with novel omnipolar electrograms. *Circ Arrhythm Electrophysiol*. 2016;9:e004107.
14. Magtibay K, Masse S, Asta J, Porta-Sanchez A, Haldar S, Malebranche D, Deno DC, Nanthakumar K. Novel ventricular voltage mapping methodology with omnipolar electrograms. *Circulation*. 2016;134:A17771 (Abstract).
15. Massé S, Sevaptisidis E, Parson ID, Kimber S, Downar E. A data acquisition system for real-time activation detection of cardiac electrograms I: hardware. *Conf Proc IEEE Eng Med Biol Soc*. 1991;13:0780–0781.
16. Massé S, Sevaptisidis E, Parson ID, Kimber S, Downar E. A data acquisition system for real-time activation detection of cardiac electrograms I: software. *Conf Proc IEEE Eng Med Biol Soc*. 1991;13:0782–0783.
17. Magtibay K, Masse S, Asta J, Lai PFH, Azam MA, Porta-Sanchez A, Haldar SK, Deno DC, Nanthakumar K. Isthmus and lesion gap: the incremental value of omnipoles over high density mapping. *Heart Rhythm* 2017;14:S528 (Abstract).
18. Sacher F, Field ME. Activation wavefront direction and the voltage map: a matter of perspective? *Circ Arrhythm Electrophysiol*. 2016;9:e004448.
19. Tung R, Josephson ME, Bradfield JS, Shivkumar K. Directional influences of ventricular activation on myocardial scar characterization: voltage mapping with multiple wavefronts during ventricular tachycardia ablation. *Circ Arrhythm Electrophysiol*. 2016;9:e004155.
20. Caldwell BJ, Trew ML, Sands GB, Hooks DA, LeGrice IJ, Smaill BH. Three distinct directions of intramural activation reveal non-uniform side-to-side electrical coupling of ventricular myocytes. *Circ Arrhythm Electrophysiol*. 2009;2:433–440.
21. Soejima K, Stevenson WG, Maisel WH, Sapp JL, Epstein LM. Electrically unexcitable scar mapping based on pacing threshold for identification of the reentry circuit isthmus: feasibility for guiding ventricular tachycardia ablation. *Circulation*. 2002;106:1678–1683.
22. Tung R, Kim S, Yagishita D, Vaseghi M, Ennis DB, Ouadah S, Shivkumar K. Scar voltage threshold determination using ex vivo magnetic resonance imaging integration in a porcine infarct model: influence of interelectrode distances and three-dimensional spatial effects of scar. *Heart Rhythm*. 2016;13:1993–2002.
23. Callans DJ, Ren JF, Michele J, Marchlinksi FE, Dillon SM. Electroanatomic left ventricular mapping in the porcine model of healed anterior myocardial infarction: correlation with intracardiac echocardiography and pathological analysis. *Circulation*. 1999;100:1744–1750.
24. Gianni C, Natale A. Voltage mapping for ventricular tachycardia ablation: we can work it out. *Heart Rhythm*. 2016;13:2003.